The Astrophysical Journal Letters, 824:L4 (7pp), 2016 June 10 doi:10.3847/2041-8205/824/1/L4

NuSTAR RESOLVES THE FIRST DUAL AGN ABOVE 10 keV IN SWIFT J2028.5+2543

Michael J. Koss[1,17], Ana Glidden[2], Mislav Baloković[3], Daniel Stern[4], Isabella Lamperti[1], Roberto Assef[5], Franz Bauer[6,7], David Ballantyne[8], Steven E. Boggs[9], William W. Craig[9,10], Duncan Farrah[11], Felix Fürst[3], Poshak Gandhi[12], Neil Gehrels[13], Charles J. Hailey[14], Fiona A. Harrison[3], Craig Markwardt[13], Alberto Masini[15], Claudio Ricci[3], Ezequiel Treister[6,16], Dominic J. Walton[3,4], and William W. Zhang[13]

[1] Institute for Astronomy, Department of Physics, ETH Zurich, Wolfgang-Pauli-Strasse 27, CH-8093 Zurich, Switzerland; mkoss@phys.ethz.ch
[2] Massachusetts Institute of Technology, 77 Massachusetts Avenue, Cambridge, MA 02139, USA
[3] Cahill Center for Astronomy and Astrophysics, California Institute of Technology, Pasadena, CA 91125, USA
[4] Jet Propulsion Laboratory, California Institute of Technology, 4800 Oak Grove Drive, Mail Stop 169-221, Pasadena, CA 91109, USA
[5] Núcleo de Astronomía de la Facultad de Ingeniería, Universidad Diego Portales, Av. Ejército 441, Santiago, Chile
[6] Instituto de Astrofísica, Facultad de Física, Pontificia Universidad Católica de Chile, Casilla 306, Santiago 22, Chile
[7] Space Science Institute, 4750 Walnut Street, Suite 205, Boulder, CO 80301, USA
[8] Center for Relativistic Astrophysics, School of Physics, Georgia Institute of Technology, Atlanta, GA 30332, USA
[9] Space Sciences Laboratory, University of California, 7 Gauss Way, Berkeley, CA 94720-7450, USA
[10] Lawrence Livermore National Laboratory, Livermore, CA 94550, USA
[11] Department of Physics, Virginia Tech, Blacksburg, VA 24061, USA
[12] School of Physics and Astronomy, University of Southampton, Highfield, Southampton SO17 1BJ, UK
[13] NASA Goddard Space Flight Center, Greenbelt, MD 20771, USA
[14] Columbia Astrophysics Laboratory, Columbia University, New York, NY 10027, USA
[15] INAF-Osservatorio Astronomico di Bologna, via Ranzani 1, I-40127 Bologna, Italy
[16] Departamento de Astronomía, Universidad de Concepción, Concepción, Chile
Received 2016 April 4; revised 2016 May 13; accepted 2016 May 13; published 2016 June 3

ABSTRACT

We have discovered heavy obscuration in the dual active galactic nucleus (AGN) in the *Swift*/Burst Alert Telescope (BAT) source SWIFT J2028.5+2543 using *Nuclear Spectroscopic Telescope Array* (*NuSTAR*). While an early *XMM-Newton* study suggested the emission was mainly from NGC 6921, the superior spatial resolution of *NuSTAR* above 10 keV resolves the *Swift*/BAT emission into two sources associated with the nearby galaxies MCG +04-48-002 and NGC 6921 ($z = 0.014$) with a projected separation of 25.3 kpc (91″). *NuSTAR*'s sensitivity above 10 keV finds both are heavily obscured to Compton-thick levels ($N_{\rm H} \approx (1\text{–}2) \times 10^{24}$ cm^{-2}) and contribute equally to the BAT detection ($L^{\rm int}_{10-50\ {\rm keV}} \approx 6 \times 10^{42}$ erg s^{-1}). The observed luminosity of both sources is severely diminished in the 2–10 keV band ($L^{\rm obs}_{2-10\ {\rm keV}} < 0.1 \times L^{\rm int}_{2-10\ {\rm keV}}$), illustrating the importance of >10 keV surveys like those with *NuSTAR* and *Swift*/BAT. Compared to archival X-ray data, MCG +04-48-002 shows significant variability (>3) between observations. Despite being bright X-ray AGNs, they are difficult to detect using optical emission-line diagnostics because MCG +04-48-002 is identified as a starburst/composite because of the high rates of star formation from a luminous infrared galaxy while NGC 6921 is only classified as a LINER using line detection limits. SWIFT J2028.5+2543 is the first dual AGN resolved above 10 keV and is the second most heavily obscured dual AGN discovered to date in the X-rays other than NGC 6240.

Key words: galaxies: active – galaxies: individual (NGC 6921, MCG +04-48-002) – galaxies: interactions – X-rays: galaxies

1. INTRODUCTION

Over the past decade, dual active galactic nuclei (AGNs) have been found serendipitously (e.g., Komossa et al. 2003; Comerford et al. 2011; Koss et al. 2011a) and also through large systematic surveys using optical spectroscopy (e.g., Liu et al. 2011; Comerford et al. 2013), X-ray emission (Koss et al. 2012; Liu et al. 2013; Comerford et al. 2015), or radio observations (Fu et al. 2015; Müller Sánchez et al. 2015). This work has suggested that close (<30 kpc) major galaxy mergers are efficient at triggering AGNs. Theorists have also suggested that AGN obscuration can rise to Compton-thick levels in the merging process ($N_{\rm H} > 10^{24}$ cm^{-2}; Hopkins et al. 2005). However, only one dual AGN has been found where both AGNs are Compton-thick: NGC 6240 (Komossa et al. 2003).

The *Swift* Burst Alert Telescope (BAT; Barthelmy et al. 2005) has proven important in nearby obscured AGN studies because it is sensitive to the 14–195 keV band, and thus to X-rays that can penetrate through even Compton-thick columns of obscuring material ($N_{\rm H} > 10^{24}$ cm^{-2}). Studies of BAT-detected AGNs have suggested that this sensitivity is linked to the high fraction of mergers and dual AGNs (Koss et al. 2010, 2012). Unfortunately, the limited angular resolution (FWHM ≈ 20′) and large positional uncertainty (≈3′; Baumgartner et al. 2013) make *Swift*/BAT ill suited for dual-AGN studies because of source confusion. With the new high-energy focusing optics on the *Nuclear Spectroscopic Telescope Array* (*NuSTAR*; Harrison et al. 2013), the 3–79 keV energy range can be studied at sensitivities and angular resolutions 10–100 times better than *Swift*/BAT. Additionally, the >10 keV sensitivity of *NuSTAR* has found intrinsic (unabsorbed) X-ray luminosities can be ≈10–70 times higher for heavily obscured sources than pre-NuSTAR constraints from *Chandra* or *XMM-Newton* (Lansbury et al. 2015).

NGC 6921 and MCG +04-48-002 were first found to host possible X-ray counterparts to SWIFT J2028.5+2543 based on *Swift*/XRT and *XMM-Newton* spectra that suggested that NGC

[17] SNSF Ambizione Fellow.

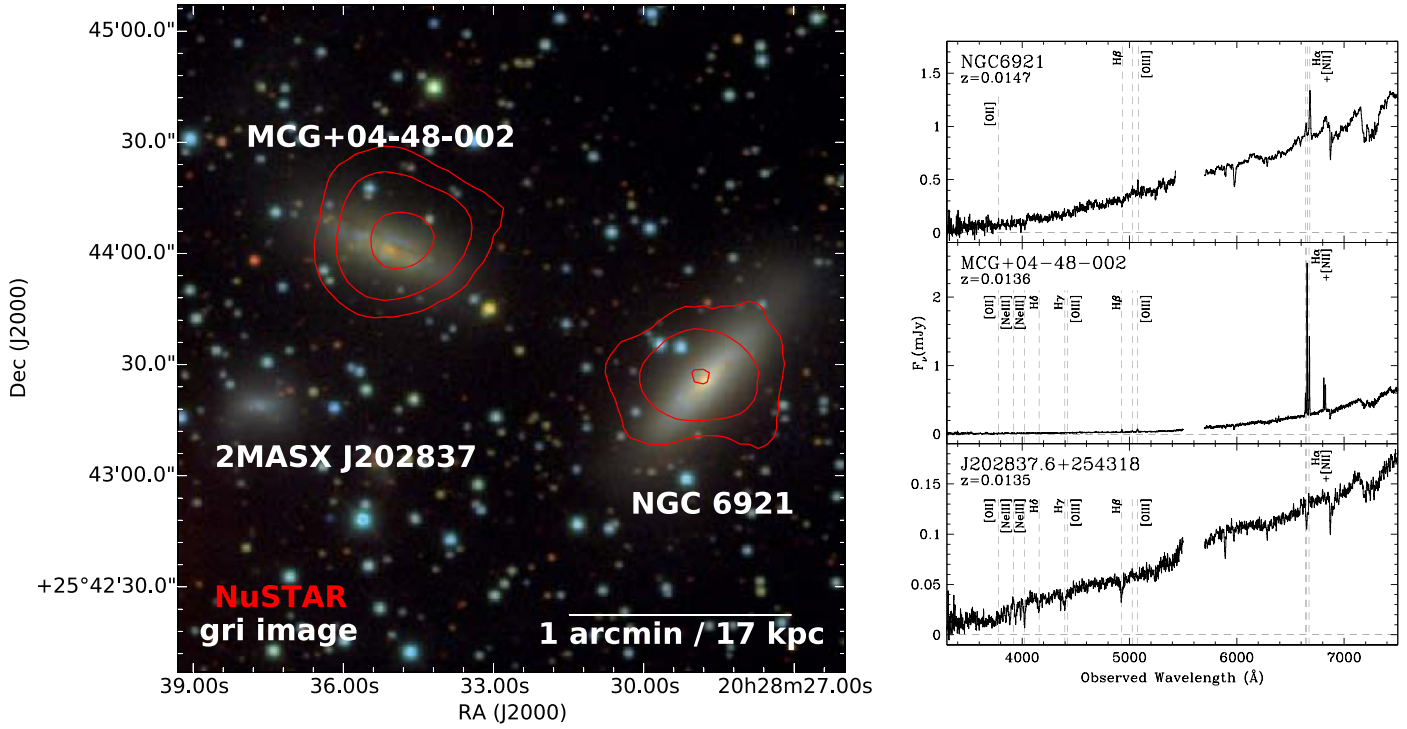

Figure 1. Left: color Kitt Peak 2.1 m optical *gri* image displayed with an arcsinh scale with *NuSTAR* X-ray (3–79 keV) contours overlaid in red. 2MASX J202837.6 +254318, the faintest galaxy in the group, is not detected by *NuSTAR*. Right: optical spectra of NGC 6921, MCG +04-48-002, and 2MASX J202837.6+254318 from Palomar. The three galaxies are found at similar redshifts, suggesting a galaxy group. Since the system is near the Galactic plane ($\delta_{\rm Gal} = -7°$), large foreground Galactic extinction (≈1 mag) and contamination by foreground stars make detection of extended merger features such as tidal tails difficult.

6921 was the primary BAT source (Winter et al. 2008) and was nearly Compton-thick ($N_{\rm H} \approx 1 \times 10^{24}\,{\rm cm}^{-2}$), while MCG +04-48-002 had a complex spectra with no evidence of obscuration. It was later classified as a dual AGN (Koss et al. 2012) based on the luminous hard X-ray emission in both AGNs ($L_{2-10\,{\rm keV}} > 10^{42}$ erg s^{-1}) and the small redshift (<500 km s^{-1}) and physical (25.2 kpc) separation between the host galaxies. A recent compilation of BAT-detected AGNs found NGC 6921 was likely Compton-thick (Ricci et al. 2015). Here, we use *NuSTAR* to resolve the >10 keV emission to find a heavily obscured dual-AGN pair in the *Swift*/BAT source SWIFT J2028.5+2543 with both sources contributing equally. Throughout this Letter, we adopt $\Omega_m = 0.3$, $\Omega_\Lambda = 0.7$, and $H_0 = 70$ km s^{-1} Mpc^{-1}.

2. OBSERVATIONS AND DATA REDUCTION

We describe here the optical imaging and spectroscopy (Section 2.1) and X-ray observations (Section 2.2). Errors are quoted at the 90% confidence level for the parameter of interest unless otherwise specified.

2.1. Optical Imaging and Spectroscopy

Optical imaging was obtained in an earlier survey of 185 BAT AGNs (*ugriz* from Koss et al. 2011b) using the Kitt Peak 2.1 m telescope. For optical spectroscopy, we used the Double Spectrograph (DBSP) on the Hale 200 inch telescope at Palomar Observatory. On UT 2013 August 13, we observed MCG +04-48-002 for 500 s with a 1.″5 slit and NGC 6921 for 300 s with a 0.″5 slit both at the parallactic angle (−68°). We also observed a nearby galaxy, 2MASX J20283767+2543183, for 600 s with a 1.″5 slit (Figure 1) on UT 2015 July 22 at the parallactic angle (58°). We processed the data with flux calibration from observations of BD +17 3248, BD +33 2642, and Feige 110. Milky Way Galactic reddening has been taken into account according to Schlafly & Finkbeiner (2011).

We use the penalized PiXel Fitting software (pPXF; Cappellari & Emsellem 2004) to measure stellar kinematics and the central stellar velocity dispersion ($\sigma_\star$) with the Indo–U. S. CaT and MILES empirical stellar library (3465–9468 Å; Vazdekis et al. 2012). We fit the residual spectra for emission lines after subtracting the stellar templates with the PYSPECKIT software following Berney et al. (2015) and correct the narrow line ratios (Hα/Hβ) assuming an intrinsic ratio of $R = 3.1$ and the Cardelli et al. (1989) reddening curve.

2.2. X-Ray Observations

A summary of the X-ray observations is given in Table 1. *NuSTAR* observed SWIFT J2028.5+2543 on 2013 May 18. The data were processed using the NuSTARDAS software version 1.4.1 and CALDB version 20150702. The exposure time totaled 19.5 ks. Rather than a single bright source, two point sources are seen in the *NuSTAR* images. For spectral extraction, we used circular regions 40″ in radius centered on the point-source peaks. A background spectrum was extracted from a polygonal region surrounding both sources. The counts totaled 780 in MCG +04-48-002 and 624 in NGC 6921. We required at least 20 counts per bin for fitting.

The *NuSTAR* observation was coordinated with a *Swift*/XRT exposure of 6.6 ks on the same day. *Swift*/XRT also observed the system three times in the past. *Swift*/XRT data were processed using the ASI Science Data Center tools. We used a 71″ circular extraction region and background extraction

Table 1
Summary of X-Ray Observations

Observatory	Observation ID	Date	Exp. (ks)	Source Count Rate[a] (s^{-1}) MCG +04-48-002/NGC 6921
Swift (XRT)	00035276001	2005 Dec 16	4.5	0.015/0.002
Swift (XRT)	00035276002	2006 Mar 23	4.6	0.013/0.004
Swift (XRT)	00030722001	2006 Jun 3	6.9	0.011/0.003
Swift (XRT)	00080266001	2013 May 18	6.6	0.005/0.003
XMM-Newton (EPIC)	0312192301	2006 Apr 23	8.8	0.150/0.035
Suzaku (XIS)	702081010	2007 Apr 18	41.3	0.026/0.008
NuSTAR	60061300002	2013 May 18	19.5	0.040/0.032
Swift (BAT)	104 month	2005–2013	10894	0.002

Note.
[a] Background-subtracted instrument count rate in: 0.3–10 keV for *Swift* (XRT) and *XMM-Newton* (EPIC), 0.1–12 keV for *Suzaku* (average between XIS0, XIS1, and XIS3), 3–79 keV for *NuSTAR* (FPMA), and 14–195 keV for *Swift* (BAT). The BAT count rate is in Crab units.

regions with inner and outer radii of 142″ and 236″, respectively, with a minimum of three counts per bin for fitting.

The system was previously observed by *XMM-Newton* and *Suzaku* on 2006 April 4 and 2007 April 18, respectively. We processed the data using standard procedures[18], employing SAS (version 7.0) for the *XMM-Newton* EPIC data and the HEAsoft script `aepipeline` for the *Suzaku* XIS data.

3. RESULTS

We first describe results from optical imaging and spectroscopy (Section 3.1), then discuss X-ray variability and spectral modeling (Sections 3.2 and 3.3). We follow with a discussion of the intrinsic AGN luminosity (Section 3.4).

3.1. Optical Imaging and Spectroscopy

A tricolor optical image (*gri*) with *NuSTAR* emission overlaid is presented in Figure 1. The [O III] λ5007 emission line is measured at ($z = 0.0136$) in MCG +04-48-002 and at ($z = 0.0147$) in NGC 6921. We also measure the Na I $\lambda\lambda$ 5890, 5896 (Na D) absorption lines from stars and cold gas since narrow emission lines in AGNs often have blueshifts compared to their hosts (Bertram et al. 2007). We measure a rest-frame velocity of 4212 ± 15 km s^{-1} ($z = 0.0139$) for MCG +04-48-002 and 4356 ± 15 km s^{-1} ($z = 0.0141$) for NGC 6921 for a ≈140 km s^{-1} offset.

There is a 91″ separation between MCG +04-48-002 and NGC 6921 that corresponds to 25.3 kpc at the [O III] line redshift in MCG +04-48-002 ($z = 0.0136$). This is slightly larger than the 25.2 kpc separation in Koss et al. (2012) because of the new DBSP spectra. Imaging shows three additional nearby extended galaxies (major axis >20″) within 360″ of MCG +04-48-002 (100 kpc), 2MASX J20283767+2543183 (15.0 kpc south), 2MASX J20285039+2545324 (62.8 kpc east), and 2MASX J20283695+2540123 (63.3 kpc south). We confirm that 2MASX J20283767+2543183 is an inactive elliptical galaxy at the same redshift ($z = 0.0135$) based on the Hβ absorption.

We find that MCG +04-48-002 is classified as a starburst using the [O I]/Hα diagnostic and a composite galaxy using the [N II]/Hα diagnostic (Figure 2; Kewley et al. 2006). MCG +04-48-002 has strong sky features in the [S II] region, so this line was not measured. NGC 6921 is classified as a LINER based on the [O I]/Hα and [S II]/Hα diagnostics and as an AGN based on [N II]/Hα. For NGC 6921, the Balmer decrement limit corresponds to $E(B - V) = 0.26$. For MCG +04-48-002, the Balmer decrement is consistent with no line obscuration (Hα/H$\beta = 2.62$).

We measure the central velocity dispersion of the Calcium triplet absorption lines to be 217 ± 9 km s^{-1} for NGC 6921 and 142 ± 10 km s^{-1} for MCG +04-48-002. Using recent scaling relations from McConnell & Ma (2013), these values correspond to $M_{\rm BH} \simeq 4 \times 10^8 M_\odot$ and $M_{\rm BH} \simeq 7 \times 10^7 M_\odot$ for NGC 6921 and MCG +04-48-002, respectively.

3.2. X-Ray Variability

We explore longer-term X-ray variability using the *Swift*/BAT 104-month data taken between 2004 and 2013 (Figure 3). The spectra of both AGNs are blended in *Swift*/BAT because of the low effective angular resolution. A χ^2 test of the full 14–195 keV band light curve, binned in one-month intervals, suggests a varying source at the >99% level. The BAT light curve shows a significant drop in count rate between the 2005–2009 period (0.0025 ± 0.0001 Crab) and the 2010–2013 period (0.0020 ± 0.0001 Crab). In *Swift*/XRT, for NGC 6921, there is no count rate variation. In contrast, MCG +04-48-002 varied significantly in the *Swift*/XRT count rate between 2013 and earlier observations in 2005 and 2006, when it was higher by a factor of ≃3, at 5σ confidence.

We then study the variability in the overlapping 3–10 keV energy range of *NuSTAR*, *XMM-Newton*, and *Suzaku*. We used `Xspec` (Arnaud 1996) version 12.8.2 for spectral analysis. We fit the X-ray data using a simple power law ($\Gamma = 1.8$) plus a normalization, a Gaussian fixed at 6.4 keV to represent the neutral Fe Kα line, and obscuration ($N_{\rm H}$) for each observation. For NGC 6921, we find no evidence of variability, with all the normalizations consistent within uncertainties. However, for MCG +04-48-002 there is significant variability in agreement with the *Swift*/XRT observations and the *Swift*/BAT data. We find that the observations from both *XMM-Newton* and *Suzaku* data show significantly higher normalizations during 2006–2007, consistent with the higher count rates in *Swift*/XRT during these times. There is also no evidence of column density variability in any of the observations. Further *NuSTAR* observations are necessary to study the unresolved high-energy variability seen by *Swift*/BAT.

[18] See http://heasarc.gsfc.nasa.gov/docs/xmm/abc/ and http://www.astro.isas.jaxa.jp/suzaku/process/.

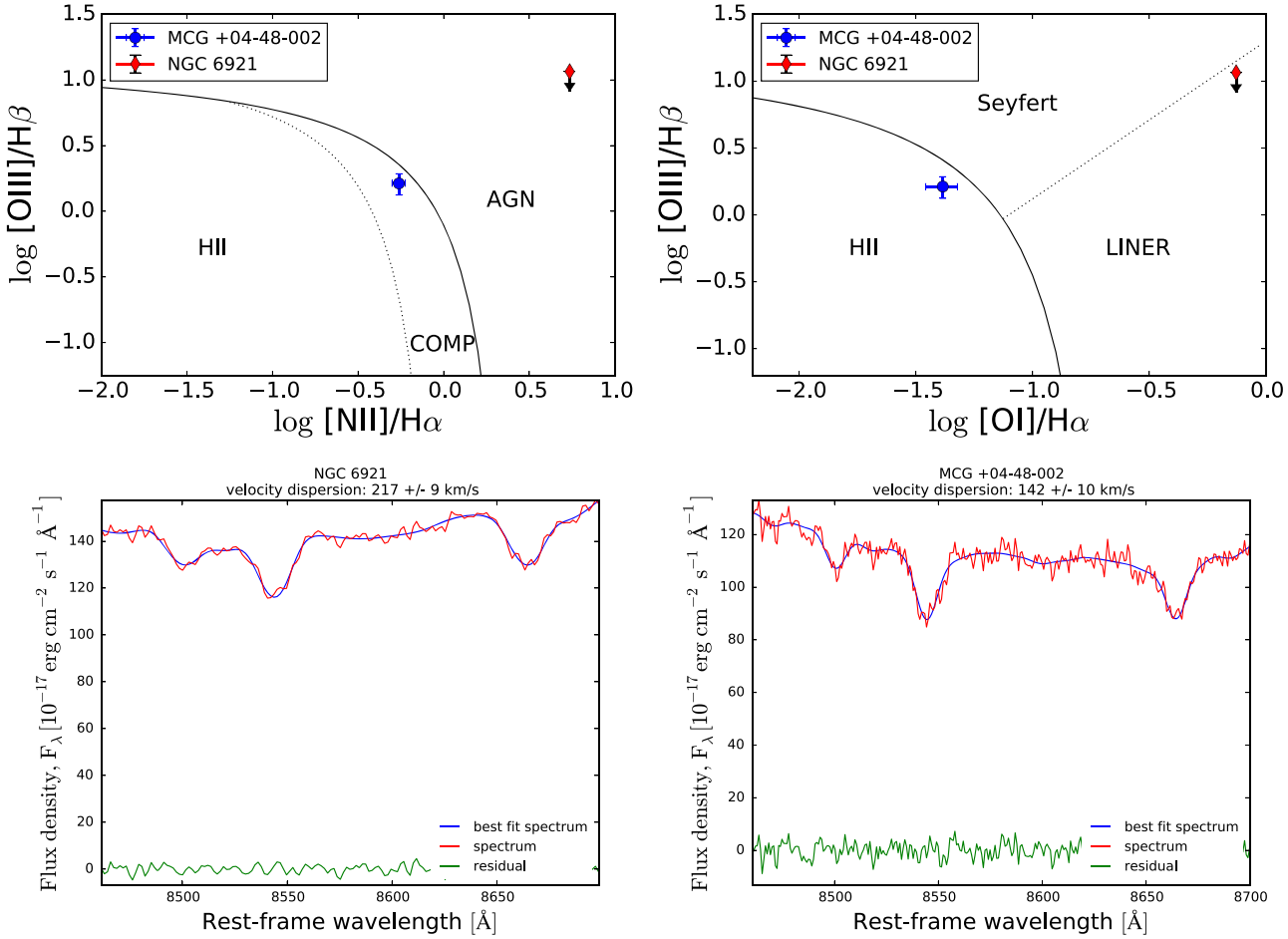

Figure 2. Emission and absorption line fits. Top: [N II]/Hα (left) and [O I]/Hα (right) diagnostic ratios (Kewley et al. 2006). The down arrows indicate Hβ line detection limits. Bottom: fits of stellar templates to the Calcium triplet region for NGC 6921 (left) and MCG +04-48-002 (right). The data are shown in red, the model in blue, and the residuals are in green.

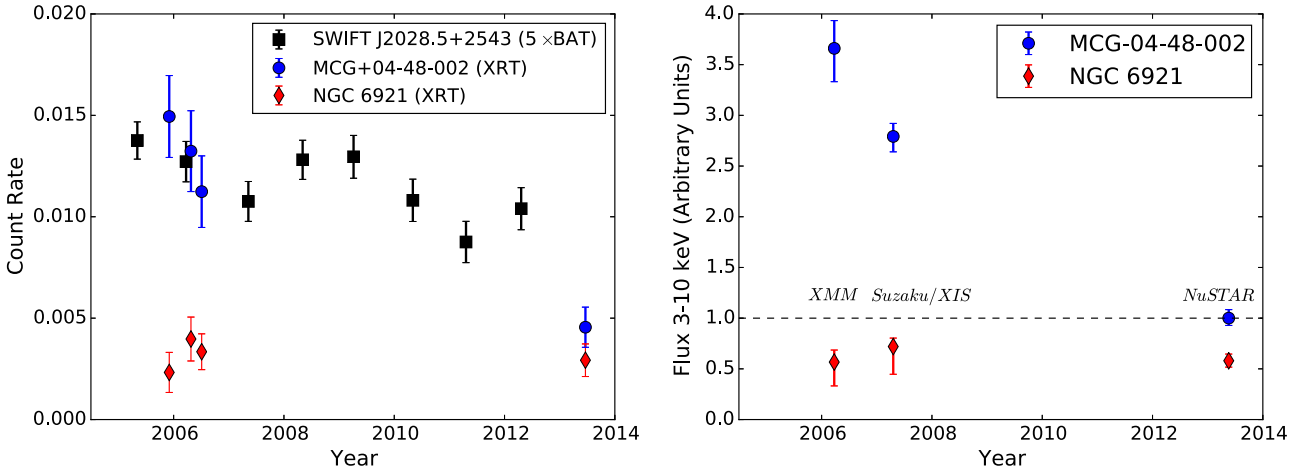

Figure 3. Left: 0.5–10 keV count rates of MCG +04-48-002 (blue) and NGC 6921 (red) from *Swift*/XRT. The BAT light curve (black) is associated with emission from both counterparts, binned into year intervals, and is normalized to the Crab. The *Swift*/BAT count rate has been rescaled by a factor of five for comparison. Right: 3–10 keV flux from MCG +04-48-002 and NGC 6921 from *XMM-Newton*, *Suzaku*, and *NuSTAR*. The horizontal dashed lines indicates the flux of MCG +04-48-002 in the recent *NuSTAR* observation.

3.3. X-Ray Spectral Fits

We first use a phenomenological model mimicking torus-obscured AGN emission to explore the spectral properties of NGC 6921 and MCG +04-48-002. This model consists of a transmission component, represented by the absorbed power-law model (including Compton scattering), a reprocessed component, represented by the disk-reprocessing model `pexrav` (Magdziarz & Zdziarski 1995) and to represent the neutral Fe Kα line emission, a Gaussian fixed at 6.4 keV. We assume a 150 keV high-energy cutoff, typical of Seyfert nuclei

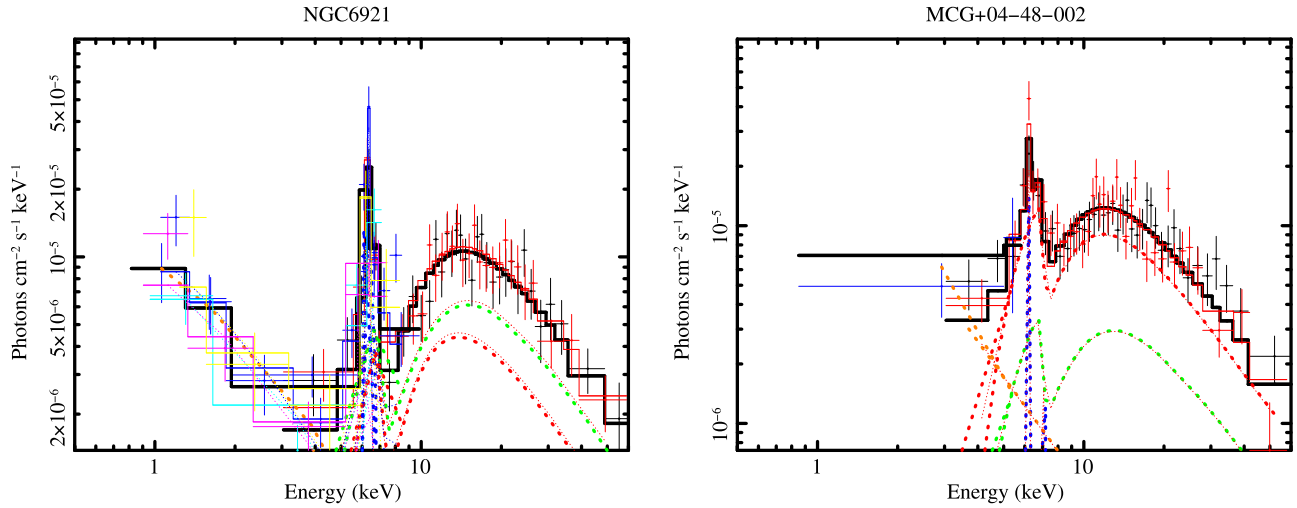

Figure 4. X-ray spectra of NGC 6921 (left) and MCG +04-48-002 (right) and best-fit `MYtorus`-based model shown binned to match the unfolded data. *NuSTAR* is shown in black (FPMA) and red (FPMB). The soft X-ray data are from *XMM-Newton* (PN-blue and MOS-yellow), *Suzaku* (magenta), and *Swift*/XRT (cyan) for NGC 6921. Since we found significant variability in MCG +04-48-002, we only use the simultaneous *Swift*/XRT observation in the soft X-rays (blue). The sum of the model is represented by a solid black line. The model components are represented by dashed lines indicating the zeroth-order transmitted continuum through photoelectric absorption (`MYTZ`, red), the scattered/reflected component (`MYTS`, green), and fluorescent emission-line spectrum (`MYTL`, dark blue). At softer energies (<3 keV), there is a model component for scattered AGN emission on larger scales in the host galaxy ($f_{\rm scatt}$, orange).

(Fabian et al. 2015). We also include a scattered power-law component with photon index equal to that of the intrinsic spectrum and relative normalization of ∼1%, as expected from Thomson scattering by the free electrons outside of the putative AGN torus. Due to the limited photon statistics, we use Cash statistics, although we also report χ^2 values due to their straightforward interpretability.

For NGC 6921, the best fit of the *NuSTAR* and *Swift*/XRT data (χ^2/dof = 36/43) is with $\Gamma = 1.8^{+0.2}_{-0.3}$ and $N_{\rm H} = (1.9 \pm 0.5) \times 10^{24}$ cm^{-2}, which corresponds to a Compton-thick scenario with the reprocessed component contributing ∼10% of the total 10–50 keV flux. This model implies an intrinsic 10–50 keV luminosity of 1.9×10^{43} erg s^{-1}. An alternative solution with slightly higher χ^2 (χ^2/dof = 47/44) is also found by allowing the reprocessed continuum to be absorbed. This implies a significantly higher column density ($\gtrsim 5 \times 10^{24}$ cm^{-2}) and a higher intrinsic luminosity (as in, e.g., Baloković et al. 2014; Brightman et al. 2015). Equivalent widths of the neutral Fe Kα line at 6.4 keV range between 0.5 and 2.4 keV, as expected from a Compton-thick torus.

The simultaneous *NuSTAR* and *Swift*/XRT spectra of MCG +04-48-002 are fitted well with the model described above (χ^2/dof = 57/49) for $\Gamma = 1.8 \pm 0.2$ and $N_{\rm H} = (1.0 \pm 0.3) \times 10^{24}$ cm^{-2}. In this solution, the relative normalization of the scattered continuum is 0.4% (<2% with 90% confidence) and the reprocessed continuum contributes 20% of the observed 10–50 keV flux (2%–130% within the 90% confidence interval). The intrinsic 10–50 keV luminosity based on this model is 6.5×10^{42} erg s^{-1}. Equivalent widths of the neutral Fe Kα line at 6.4 keV are 0.3–1.2 keV. If we include the archival soft X-ray data assuming a normalization offset because the source was significantly brighter, the $N_{\rm H} = (8 \pm 3) \times 10^{23}$ cm^{-2}, suggesting that the column density did not change drastically between observations though the lack of >10 keV coverage in the earlier observation limits our constraints.

Following the strategies of past studies of single AGNs observed with *NuSTAR* (e.g., Baloković et al. 2014; Gandhi et al. 2014; Koss et al. 2015), we fit the X-ray spectra with the `MYtorus`model (Murphy & Yaqoob 2009) shown in Figure 4. For NGC 6921 we combine the *Suzaku*, *XMM-Newton*, and *Swift*/XRT data, with an offset of 10% variability allowed for telescope cross-normalization. We find $\Gamma = 1.7 \pm 0.1$, $N_{\rm H} = (1.4 \pm 0.1) \times 10^{24}$ cm^{-2}, and $\theta_{\rm inc} = 89^{\circ}{}^{+1}_{-8}$, consistent with a Compton-thick torus observed nearly edge-on (χ^2/dof = 67/79). Using this model we find $L^{\rm obs/int}_{2-10\ {\rm keV}} = (0.3/4.4) \times 10^{42}$ erg s^{-1} and $L^{\rm obs/int}_{10-50\ {\rm keV}} = (3.6/5.5) \times 10^{42}$ erg s^{-1} for NGC 6921. For MCG +04-48-002, we limit our fit to the simultaneous *NuSTAR* and *Swift*/XRT spectra because of variability. Using the `MYtorus`model with fixed $\Gamma = 1.9$, $\theta_{\rm inc} = 85^{\circ}$, and $\theta_{\rm tor} = 60^{\circ}$, we obtain a column density of $N_{\rm H} = 1.0^{+0.4}_{-0.2} \times 10^{24}$ cm^{-2}, in agreement with our simpler model (χ^2/dof = 64/83). We find $L^{\rm obs/int}_{2-10\ {\rm keV}} = (0.2/3.7) \times 10^{42}$ erg s^{-1} and $L^{\rm obs/int}_{10-50\ {\rm keV}} = (3.2/6.1) \times 10^{42}$ erg s^{-1} with this model.

3.4. Intrinsic Luminosity and Eddington Ratio

One estimate of the intrinsic AGN luminosity comes from [O III]. The [O III] luminosity is 1.1×10^{39} erg s^{-1} for NGC 6921 and 1.5×10^{39} erg s^{-1} for MCG +04-48-002. Based on the relation from a study of 351 BAT AGNs (Berney et al. 2015), we expect $L_{[\rm O\ III]} \simeq 4.9 \times 10^{40}$ erg s^{-1} for NGC 6921 and $L_{[\rm O\ III]} \simeq 4.0 \times 10^{40}$ erg s^{-1} for MCG +04-48-002 as inferred from the 2–10 keV intrinsic luminosity derived from the X-ray spectra. This values are 25–45 times higher than observed, implying both sources have weak [O III] emission, though some extended [O III] is likely missed because the slit widths correspond to ≈150 pc and ≈450 pc for NGC 6921 and MCG +04-48-002, respectively.

Another estimate of intrinsic AGN luminosity is $L_{12\ \mu{\rm m}}$ which is measured using the photometry from the *Wide-field Infrared Survey Explorer* final catalog release at 7.0×10^{42} erg s^{-1} for NGC 6921, and 3.0×10^{43} erg s^{-1} for MCG +04-48-002. The expected unabsorbed 2–10 keV luminosity, based upon the mid-IR/X-ray correlation is then

$\simeq 1.5 \times 10^{43}$ erg s^{-1} in NGC 6921 and $\simeq 6.2 \times 10^{43}$ erg s^{-1} in MCG +04-48-002 (Gandhi et al. 2009; Asmus et al. 2015). The estimate of intrinsic AGN luminosity of MCG +04-48-002 from $L_{12\,\mu m}$ is then more than a factor of three higher than our X-ray measurement, suggesting we underestimated the intrinsic luminosity in the X-rays and MCG +04-48-002 may be heavily Compton-thick. We note, however, that some of the IR emission may be from star formation from MCG +04-48-002 being a luminous infrared galaxy (LIRG; Armus et al. 2009).

We use a bolometric correction of 15 (Vasudevan & Fabian 2009) to convert the unabsorbed 2–10 keV luminosities to bolometric luminosities. This implies a bolometric luminosity of $\simeq 7 \times 10^{43}$ erg s^{-1} for NGC 6921 and 6×10^{43} erg s^{-1} for MCG +04-48-002. Combined with the measured SMBH mass we estimate the Eddington fraction, $L_{\rm Bol}/L_{\rm Edd}$, where $L_{\rm Edd}$ is the Eddington luminosity. The Eddington ratio is then $\approx$0.001 for NGC 6921 and $\approx$0.009 for MCG +04-48-002.

4. DISCUSSION

We have discovered heavy obscuration in the dual AGN associated with the *Swift*/BAT source SWIFT J2028.5+2543 using *NuSTAR*. NGC 6921 is obscured by a Compton-thick column that is well constrained by the *NuSTAR* data, but only poorly constrained by the archival soft X-ray data. MCG +04-48-002 is obscured by heavy to Compton-thick material along the line of sight ($N_{\rm H} \approx 1 \times 10^{24}$ cm^{-2}), with deeper observations required to better understand the variability. Both sources are severely diminished in the 2–10 keV band ($L^{\rm obs/int}_{2-10\,\rm keV} < 0.1$) while the majority of the >10 keV emission is detected, illustrating the importance of *NuSTAR* and *Swift*/BAT. On average, the two AGNs are similarly luminous (within a factor of $\simeq$2). We note that in Winter et al. (2008) an error was likely made in identifying the two sources in the *XMM-Newton* image, such that their names were switched. This led Winter et al. (2009) to claim that NGC 6921 was highly variable between the *XMM-Newton* and *Suzaku* observations. However, from our results it is clear that MCG +04-48-002 is brighter in the observed 0.5–10 keV emission than NGC 6921 in all X-ray observations and NGC 6921 shows no significant evidence of variability between observations.

Despite being bright, nearby X-ray selected AGNs, these sources would be missed in large optical spectroscopic AGN catalogs (e.g., Kauffmann et al. 2003). For NGC 6921, high levels of dust extinction likely contribute to the Hβ non-detection, and for the LIRG MCG +04-48-002, the intense star formation may overwhelm the AGN photoionization signature. This is typical of about 5% of BAT-selected AGNs (Smith et al. 2014; Schawinski et al. 2015) and is more common to BAT-selected AGNs in ongoing mergers that tend to have lower [O III]/X-ray ratios (Koss et al. 2010).

The pair shows spectroscopic signatures typical of merger-triggered dual AGNs rather than a chance association. The small line of sight velocity offset ($\simeq$140 km s^{-1}) is typical of dual AGNs found using other techniques (50–300 km s^{-1}; Comerford et al. 2013). AGNs bright enough to be detected by *Swift*/BAT are rare (e.g., 0.02 per square degree on the sky; Baumgartner et al. 2013). Since there are only three other nearby ($\pm$200 km s^{-1}) BAT sources of MCG +04-48-002 in the entire sky, the chance possibility of a random BAT AGN at the same redshift within 91″ is very small ($<10^{-8}$). Since the system is near the Galactic plane ($\delta_{\rm Gal} = -7°$), large foreground Galactic extinction ($\approx$1 mag) makes optical detection of merger features like tidal tails difficult. Mapping the distribution and line of sight velocity of the atomic gas in the 21 cm line of neutral hydrogen to search for gas-rich material thrown off in such encounters (e.g., Hibbard & van Gorkom 1996) would be helpful for studying the merger. However, no sufficiently high-resolution maps currently exist from all-sky surveys for this sky region.

The heavily obscured dual AGNs in MCG +04-48-002 and NGC 6921 share several properties with the BAT-detected Compton-thick dual-AGN NGC 6240. Both systems are LIRGs, which are rare in the nearby universe ($z < 0.03$) and in the BAT sample (Koss et al. 2013). The intrinsic 2–10 keV luminosities of the dual AGNs are nearly equal, which is similar to NGC 6240 (Puccetti et al. 2016), but not common in typical BAT-detected dual AGNs where the median ratio is 11 (Koss et al. 2012). NGC 6240 is also classified as a LINER, similar to NGC 6921, which is found in only $\approx$4% of the BAT sample (M. Koss et al. 2016, in preparation). NGC 6240, however, is at a 1.4 kpc separation, whereas this system has a larger 25.3 kpc separation, suggesting even the early merger phase (20–30 kpc) can contribute to both AGNs' obscuration. Larger statistical studies to understand merger-triggered obscuration with *NuSTAR* are currently being performed in BAT AGNs (M. Koss et al. 2016, submitted) and in LIRGs (C. Ricci et al. 2016, in preparation).

We acknowledge the Ambizione fellowship grant PZ00P2_154799/1 (MK) and the Joanna Wall Muir and the Caltech Student Faculty Program (AG). This work was supported under NASA Contract No. NNG08FD60C and made use of *NuSTAR* mission data, a project led by the California Institute of Technology and managed by the Jet Propulsion Laboratory.

Facilities: Swift, KPNO:2.1m, Hale, *NuSTAR*, *XMM*, *Suzaku*.

REFERENCES

Armus, L., Mazzarella, J. M., Evans, A. S., et al. 2009, PASP, 121, 559
Arnaud, K. A. 1996, in ASP Conf. Ser. 101, Astronomical Data Analysis Software and Systems, ed. G. H. Jacoby, & J. Barnes (San Francisco, CA: ASP), 17
Asmus, D., Gandhi, P., Hoenig, S. F., Smette, A., & Duschl, W. J. 2015, MNRAS, 454, 766
Baloković, M., Comastri, A., Harrison, F. A., et al. 2014, ApJ, 794, 111
Barthelmy, S. D., Barbier, L. M., Cummings, J. R., et al. 2005, SSRv, 120, 143
Baumgartner, W. H., Tueller, J., Markwardt, C. B., et al. 2013, ApJS, 207, 19
Berney, S., Koss, M., Trakhtenbrot, B., et al. 2015, MNRAS, 454, 3622
Bertram, T., Eckart, A., Fischer, S., et al. 2007, A&A, 470, 571
Brightman, M., Baloković, M., Stern, D., et al. 2015, ApJ, 805, 41
Cappellari, M., & Emsellem, E. 2004, PASJ, 116, 138
Cardelli, J. A., Clayton, G. C., & Mathis, J. S. 1989, ApJ, 345, 245
Comerford, J. M., Pooley, D., Barrows, R. S., et al. 2015, ApJ, 806, 219
Comerford, J. M., Pooley, D., Gerke, B. F., & Madejski, G. M. 2011, ApJL, 737, L19
Comerford, J. M., Schluns, K., Greene, J. E., & Cool, R. J. 2013, ApJ, 777, 64
Fabian, A. C., Lohfink, A., Kara, E., et al. 2015, MNRAS, 451, 4375
Fu, H., Myers, A. D., Djorgovski, S. G., et al. 2015, ApJ, 799, 72
Gandhi, P., Horst, H., Smette, A., et al. 2009, A&A, 502, 457
Gandhi, P., Lansbury, G. B., Alexander, D. M., et al. 2014, ApJ, 792, 117
Harrison, F. A., Craig, W. W., Christensen, F. E., et al. 2013, ApJ, 770, 103
Hibbard, J. E., & van Gorkom, J. H. 1996, AJ, 111, 655
Hopkins, P. F., Hernquist, L., Martini, P., et al. 2005, ApJL, 625, L71
Kauffmann, G., Heckman, T. M., Tremonti, C., et al. 2003, MNRAS, 346, 1055
Kewley, L. J., Groves, B., Kauffmann, G., & Heckman, T. 2006, MNRAS, 372, 961
Komossa, S., Burwitz, V., Hasinger, G., et al. 2003, ApJL, 582, L15

Koss, M., Mushotzky, R., Baumgartner, W., et al. 2013, ApJL, 765, L26
Koss, M., Mushotzky, R., Treister, E., et al. 2011a, ApJL, 735, L42
Koss, M., Mushotzky, R., Treister, E., et al. 2012, ApJL, 746, L22
Koss, M., Mushotzky, R., Veilleux, S., & Winter, L. 2010, ApJL, 716, L125
Koss, M., Mushotzky, R., Veilleux, S., et al. 2011b, ApJ, 739, 57
Koss, M. J., Romero-Cañizales, C., Baronchelli, L., et al. 2015, ApJ, 807, 149
Lansbury, G. B., Gandhi, P., Alexander, D. M., et al. 2015, ApJ, 809, 115
Liu, X., Civano, F., Shen, Y., et al. 2013, ApJ, 762, 110
Liu, X., Shen, Y., Strauss, M. A., & Hao, L. 2011, ApJ, 737, 101
Magdziarz, P., & Zdziarski, A. A. 1995, MNRAS, 273, 837
McConnell, N. J., & Ma, C.-P. 2013, ApJ, 764, 184
Müller Sánchez, F., Comerford, J. M., Nevin, R., et al. 2015, ApJ, 813, 103
Murphy, K. D., & Yaqoob, T. 2009, MNRAS, 397, 1549
Puccetti, S., Comastri, A., Bauer, F. E., et al. 2016, A&A, 585, A157
Ricci, C., Ueda, Y., Koss, M. J., et al. 2015, ApJL, 815, L13
Schawinski, K., Koss, M., Berney, S., & Sartori, L. F. 2015, MNRAS, 451, 2517
Schlafly, E. F., & Finkbeiner, D. P. 2011, ApJ, 737, 103
Smith, K. L., Koss, M., & Mushotzky, R. F. 2014, ApJ, 794, 112
Vasudevan, R. V., & Fabian, A. C. 2009, MNRAS, 392, 1124
Vazdekis, A., Ricciardelli, E., Cenarro, A. J., et al. 2012, MNRAS, 424, 157
Winter, L., Mushotzky, R., Tueller, J., & Markwardt, C. 2008, ApJ, 674, 686
Winter, L. M., Mushotzky, R. F., Reynolds, C. S., & Tueller, J. 2009, ApJ, 690, 1322